Research Square

Preprints are preliminary reports that have not undergone peer review.
They should not be considered conclusive, used to inform clinical practice,
or referenced by the media as validated information.

Chemical Composition and Antimicrobial Activity of Aerial Parts Essential Oils from Three Turkish Heracleum Species

Damla Kırcı
Izmir Kâtip Çelebi University
Ayla Kaya
aykaya@anadolu.edu.tr
Anadolu University
Betül Demirci
Anadolu University
Süleyman Doğu
Meram Vocational School, Necmettin Erbakan University

Research Article

Keywords: Heracleum, essential oil, GC-MS, antimicrobial activity, molecular docking

Posted Date: November 9th, 2026

DOI: https://doi.org/10.21203/rs.3.rs-11328214/v1

License: This work is licensed under a Creative Commons Attribution 4.0 International License.
Read Full License

Additional Declarations: No competing interests reported.

Chemical Composition and Antimicrobial Activity of Aerial Parts Essential Oils from Three Turkish *Heracleum* Species

Damla Kırcı[a] Ayla Kaya[*,b], Betül Demirci[c], and Süleyman Doğu[d]

[a] Department of Pharmacognosy, Faculty of Pharmacy, İzmir Kâtip Çelebi University, İzmir, Türkiye.

[b*] Department of Pharmaceutical Botany, Faculty of Pharmacy, Anadolu University, Eskişehir, Türkiye; e-mail: aykaya@anadolu.edu.tr

[c] Department of Pharmacognosy, Faculty of Pharmacy, Anadolu University, Eskişehir, Türkiye.

[d] Department of Medical and Aromatic Plants, Meram Vocational School, Necmettin Erbakan University, Konya, Türkiye.

Damla Kırcı: https://orcid.org/0000-0002-3479-3999

Ayla Kaya: https://orcid.org/0000-0002-7598-7132

Betül Demirci: https://orcid.org/0000-0003-2343-746X

Süleyman Doğu: https://orcid.org/000-0002-5352-9288

Abstract: The genus *Heracleum* (Apiaceae) comprises aromatic plants traditionally used in folk medicine for various ailments, particularly digestive complaints. This study aimed to characterize the chemical composition and antimicrobial potential of essential oils obtained from the aerial parts of *H. argaeum, H. platytaenium,* and *H. sphondylium* subsp. *ternatum*, supported by multivariate analysis and *in silico* investigations. Essential oils were analysed using GC-FID/GC-MS, and their antimicrobial activities were evaluated experimentally. Multivariate analysis, molecular docking against fungal CYP51, and ADMET predictions were performed to investigate chemical variability and the pharmacological potential of selected constituents. Essential oil yields ranged from 0.07 to 0.18% (v/w), with identified constituents representing 95.1-98.8% of the oils. *H. argaeum* exhibited a mixed monoterpene-ester profile, whereas *H. platytaenium* and *H. sphondylium* subsp. *ternatum* were dominated by hexyl butyrate and octyl acetate, respectively. The first detailed relative-percentage compositional profile of *H. argaeum* aerial-part oil was established. All oils showed their strongest antimicrobial activity against *Candida krusei*, with *H. argaeum* exhibiting the lowest MIC (1.25 mg/mL). *(-)*-Limonene demonstrated the most favorable predicted CYP51 binding affinities, mainly through hydrophobic interactions. ADMET predictions indicated high intestinal absorption and no AMES, hepatotoxicity, or hERG alerts, although four constituents showed skin-sensitisation alerts. These findings expand knowledge of the chemical diversity of Heracleum essential oils and provide a basis for further experimental investigation of their antifungal potential.

Keywords: *Heracleum*; essential oil; GC-MS; antimicrobial activity; molecular docking

Introduction

The genus *Heracleum* L. belongs to the family Apiaceae and the tribe Tordylieae and comprises more than 120 species, making it one of the largest genera within Apiaceae. Its members are distributed predominantly throughout the Northern Hemisphere, particularly in Eurasia, and include tall or dwarf perennial and monocarpic aromatic herbs. The leaves may be simple and lobed, pinnate, trisect, or biternate; the petals are generally white or occasionally pale greenish, whereas the fruits may be spiny or comparatively small and glabrous. This marked morphological diversity contributes to the taxonomic complexity of the genus (Davis, 1972; Bahadori et al., 2016).

Ethnobotanically, *Heracleum* species have long been used as both foods and medicinal plants across Europe and Asia. Young shoots, leaves, stems, and fruits are variously consumed as vegetables, pickles, teas, spices, flavoring agents, food additives, or liqueur ingredients, while their traditional medicinal applications include the management of flatulence, stomachache, diarrhea, dysentery, epilepsy, pain, wounds, digestive disorders, and menstrual complaints, as well as their use as carminative, antiseptic, sedative, analgesic, anticonvulsant, and antihypertensive remedies (Bahadori et al., 2016).

Heracleum argaeum Boiss. & Bal. is a Turkish endemic taxon, 30-55 cm tall, distinguished by ternate-to-pinnate lower leaves with sessile, suborbicular-to-reniform terminal segments, 7-11 unequal umbel rays, and fruits lacking commissural vittae (Fırat, 2024). Previous phytochemical investigations of this species have focused primarily on its essential oil. GC-MS analysis of the major compound of fruit EO identified as hexyl butyrate (39.1%) (Baser et al., 1998). Albayrak et al. reported that the flowering aerial parts yielded 1.74% (v/w) essential oil containing several identified constituents without quantitative abundance data, while the methanol extract contained 17.74±0.40 mg GAE/g total phenolics and 11.28±0.10 mg QE/g total flavonoids, exhibited antioxidant activity, and concentration-dependently inhibited eight of the thirteen tested bacterial strains (Albayrak et al., 2014).

Heracleum platytaenium Boiss. is a Turkish endemic species particularly associated with the Ida Mountains. Its leaves and fruits are prepared as tea and traditionally used in the treatment of gastritis, enteritis, and epilepsy. Phytochemical

investigation of its aerial parts afforded the furocoumarins psoralen, bergapten, xanthotoxin, pimpinellin, isopimpinellin, sphondin, byakangelicin, heraclenol, and apterin, together with the phytosterol stigmasterol (Diçel et al., 2013). Fruit oils obtained using different isolation techniques were dominated by octyl acetate (84.8-87.8%), whereas an aerial part of essential oil (EO) similarly contained octyl acetate (85.53%) (Özek et al., 2005; Akçın et al., 2013). Biologically, the aerial part of EO strongly inhibited *Candida glabrata*, producing inhibition zones of 12-32 mm without detectable activity against the tested bacteria, while pimpinellin showed 78.57±2.86% acetylcholinesterase and 82.17±1.66% butyrylcholinesterase inhibition at 200 µg/mL (Dinçel et al., 2013; Akçın et al., 2013).

Heracleum sphondylium subsp. *ternatum* belongs to the morphologically variable *H. sphondylium* complex, which exhibits marked variation in leaf-blade division and flower color and is generally characterized by terminal umbels bearing enlarged outer petals (Matarrese and Renna, 2023). At the species level, *H. sphondylium* has been consumed as food and traditionally used for hypertension, diarrhea, dysentery, wound healing, dyspepsia, and menstrual complaints, as well as a sedative, stomachic, digestive, and aphrodisiac remedy (Bahadori et al., 2016). Non-volatile investigations of subsp. *ternatum* revealed a high abundance of chlorogenic acid in the aerial parts methanol extract, while HPLC analysis of the roots identified xanthotoxin and bergapten (Uysal et al., 2019; Kurtul et al., 2025). Essential oil studies have focused mainly on seeds and fruits: the seed oil was rich in 1-octanol (50.3%) and octyl butyrate (24.6%), whereas fruit oils varied according to isolation method and geographical origin but were consistently characterized by octyl butyrate (10.1-42.9%) and octyl acetate (10.6-60.2%) (Özek et al., 2002; İşcan et al., 2003; Maggi et al., 2014). Biologically, 1-octanol was identified by bioautography as an active antimicrobial constituent of seed oil; the fruit oil displayed cytotoxicity against A375 melanoma and HCT116 colon carcinoma cells, with octyl butyrate being chiefly responsible for this effect; and the root extracts showed significant anti-inflammatory activity (İşcan et al., 2003; Maggi et al., 2014; Kurtul et al., 2025).

The present study aimed to characterize and comparatively evaluate the essential oils obtained from the aerial parts of *H. argaeum*, *H. platytaenium*, and *H. sphondylium* subsp. *ternatum*. GC-FID and GC-MS analyses of the oils were performed, and their shared and taxon-specific constituents were assessed using Venn, PCA, and HCA analyses. The antimicrobial activities of the oils were evaluated against selected Gram-positive and Gram-negative bacteria and *Candida* strains, while the possible interactions of their major volatile compounds with the lanosterol 14α-demethylase enzymes of *Candida albicans* and *Candida krusei* were investigated by molecular docking. In addition, the physicochemical and predicted ADMET properties of major compounds were evaluated to provide further insight into their potential pharmacological relevance.

Results and Discussion

Extraction Yield and Essential Oil Composition

Essential oils (EOs) of *Heracleum* species were analyzed by both GC-MS and GC-FID simultaneously. The chemical compositions are given in **Table 1**. Hydrodistillation of the aerial parts yielded 0.07%, 0.10%, and 0.18% (v/w) essential oil for *Heracleum argaeum, H. platytaenium, and H. sphondylium* subsp. *ternatum*, respectively. GC-FID and GC-MS analyses identified 60 constituents in *H. argaeum*, accounting for 95.1% of the oil. This oil exhibited a monoterpene-rich profile dominated by α-pinene (15.0%), β-pinene (9.0%), limonene (8.9%), and together hexyl butyrate (8.3%). In *H. platytaenium,* 54 constituents represented 98.8% of the total oil. Its composition was characterised mainly by hexyl butyrate (40.8%) and octyl acetate (13.7%). The EO of *H. sphondylium* subsp. *ternatum* contained 43 identified constituents, corresponding to 98.0% of the EO, and octyl acetate (53.6%) and octyl butyrate (18.5%) are main compounds. Thus, the

three EOs differed not only in yield but also in their main chemical classes: *H. argaeum* was characterised primarily by monoterpenes, whereas the other two oils were dominated by aliphatic esters.

Table 1. The chemical composition of essential oils of *Heracleum* species

RRI	Compound	HA (%)	HP (%)	HS (%)	IM
952	1-Nonene	0.5	-	-	MS
970	Isopropyl isobutyrate	-	0.5	-	MS
1051	Isopropyl butyrate	-	0.1	-	MS
1032	*α*-Pinene	**15.0**	-	0.1	RRI, MS
1061	Isopropyl 2-methyl-butyrate	-	0.8	-	MS
1076	Camphene	3.5	-	-	RRI, MS
1083	Isopropyl isovalerate	-	1.7	0.1	MS
1093	Hexanal	-	0.1	0.1	RRI, MS
1118	*β*-Pinene	**9.0**	tr	tr	RRI, MS
1132	Sabinene	0.4	0.1	-	RRI, MS
1151	Propyl 2-methylbutyrate	-	0.1	-	MS
1159	Butyl isobutyrate	-	0.3	-	MS
1167	Propyl isovalerate	-	0.2	-	MS
1170	Isobutyl butyrate	0.3	0.9	-	MS
1174	Myrcene	2.6	-	-	RRI, MS
1185	Isobuthyl 2-methylbutyrate	0.2	0.3	-	MS
1194	Heptanal	-	-	0.1	RRI, MS
1198	Isobutyl isovalerate	-	0.3	tr	MS
1203	2-Methylbutyl isobutyrate	-	0.2	-	MS
1203	Limonene	**8.9**	-	-	RRI, MS
1218	*β*-Phellandrene	0.2	-	-	RRI, MS
1230	*n*-Butyl-*n*-butyrate	1.3	1.1	-	MS
1241	Butyl 2-methylbutyrate	-	0.6	0.1	MS
1244	2-Pentyl furan	-	-	tr	MS
1246	*(Z)- β*-Ocimene	5.1	-	0.3	MS
1255	*γ*-Terpinene	2.0	2.7	-	RRI, MS
1259	Butyl isovalerate	-	0.7	0.2	MS
1266	*(E)- β*-Ocimene	6.1	-	-	MS
1276	2-Methyl butylbutyrate	0.4	0.4	-	MS
1280	*p*-Cymene	1.4	2.3	0.1	RRI, MS
1282	Hexyl acetate	0.2	0.4	0.1	RRI, MS
1286	Isoamyl isovalerate	0.2	0.2	0.1	MS
1286	2-Methylbutyl 3-methyl-butyrate	-	-	0.3	MS
1290	Terpinolene	1.0	-	-	RRI, MS
1296	Octanal	0.1	1.1	1.8	MS

1303	2-Methylbutyl isovalerate	0.1	0.1	-	MS
1348	6-Methyl-5-hepten-2-one	0.1	-	-	MS
1350	Hexyl propionate	-	0.5	0.1	MS
1353	Hexyl isobutyrate	0.3	5.0	0.1	MS
1360	1-Hexanol	-	-	0.2	RRI, MS
1382	Alloosimene	0.1	-	-	MS
1384	Heptyl acetate	-	-	tr	MS
1400	Nonanal	-	0.1	0.1	MS
1424	Hexyl butyrate (=hexyl butanoate)	**8.3**	**40.8**	0.3	MS
1438	Hexyl 2-methyl butyrate	0.5	5.3	0.3	MS
1457	Hexyl isovalerate	-	0.4	0.5	MS
1482	Octyl acetate	1.0	**13.7**	**53.6**	RRI, MS
1506	Decanal	0.1	0.4	0.3	MS
1516	*(Z)*-4-Octenyl acetate	0.1	2.0	3.8	MS
1535	*β*-Bourbonone	0.3	-	-	MS
1547	*(Z)*-4-Decenal	-	0.1	-	MS
1547	Octyl isobutyrate	0.1	1.8	-	MS
1553	Linalool	0.1	-	-	RRI, MS
1562	Octanol	1.7	1.1	3.5	RRI, MS
1571	Pentyl hexanoate	-	0.2	-	MS
1583	*(Z)*-4-Octenyl isobutyrate	-	0.1	-	MS
1590	Bornyl acetate	7.8	-	-	RRI, MS
1612	*β*-Caryophyllene	0.4	-	0.3	RRI, MS
1617	Lavandulyl acetate	0.4	-	-	RRI, MS
1617	Hexyl hexanoate	0.2	3.5	-	MS
1624	Octyl butyrate	0.6	2.8	**18.5**	MS
1634	Octyl 2-methyl butyrate	0.3	2.7	0.1	MS
1655	Octyl isovalerate	-	0.2	0.2	MS
1661	*(Z)*-4-Octenyl butyrate	-	0.3	1.1	MS
1668	*(Z)*-*β*-Farnesene	1.0	-	-	MS
1668	Citronellyl acetate	0.2	-	-	RRI, MS
1671	*(Z)*-4-Octenyl-2-methyl-butyrate	0.8	0.3	0.4	MS
1683	*trans*-Verbenol	0.2	-	-	RRI, MS
1687	Methyl chavicol	1.2	-	-	MS
1690	Decyl acetate	-	-	0.4	RRI, MS
1700	*p*-Mentha-1,8-dien-4-ol (=*Limonen-4-ol*)	0.1	-	-	RRI, MS
1709	*α*-Terpinyl acetate	0.7	-	-	RRI, MS
1786	ar-Curcumene	-	0.1	-	MS
1786	Kessane	0.2	-	-	MS

1815	Hexyl octanoate	-	0.1	-	MS
1829	Octyl hexanoate	0.3	0.8	0.2	MS
1830	Decyl butyrate	-	-	0.1	MS
1845	*(E)*-Anethol	0.2	-	-	RRI, MS
1864	*p*-Cymen-8-ol	0.2	-	-	MS
1868	*(E)*-Geranyl acetone	0.3	-	-	MS
1988	2-Phenylethyl 2-methylbutyrate	0.4	-	-	MS
1992	2-Phenylethyl 3-methylbutyrate	0.1	-	-	MS
2008	Caryophyllene oxide	0.3	0.1	0.3	RRI, MS
2020	Octyl octanoate	-	0.5	-	MS
2041	Pentadecanal	-	0.1	-	MS
2050	*(E)*-Nerolidol	0.5	-	-	MS
2131	Hexahydrofarnesyl acetone	-	-	0.2	MS
2144	Spathulenol	0.8	0.2	-	MS
2209	*T*-Muurolol	-	0.1	-	MS
2245	Elemicin	-	-	0.3	MS
2255	*α*-Cadinol	-	0.2	-	MS
2296	Myristicin	0.6	-	7.9	RRI, MS
2330	(*2E,6Z*)-Farnesol	0.2	-	-	MS
2369	Eudesma-4(15)7-dien-1-*β*-ol	-	0.1	-	MS
2515	Apiole	-	-	1.6	MS
2551	Geranyl linalool	5.5	-	-	MS
2607	1-Octadecanol	-	-	0.2	MS
2655	Benzyl benzoate	0.4	-	-	RRI, MS
2931	Hexadecanoic acid	-	-	tr	RRI, MS
	Yield	**0.07**	**0.1**	**0.18**	
	Total	**95.1**	**98.8**	**98.0**	

HA: *Heracleum argaeum*; **HP**: *H. platytaenium;* **HS:** *H. sphondylium* subsp. *Ternatum;* **RRI:** Relative retention indices calculated against *n*-alkanes; **%**: calculated from FID data; mean % calculated from Flame Ionization Detector (FID) data; **tr:** Trace (<0.1 %); Identification method based on the relative retention indices (RRI) of authentic compounds on a HP Innowax column; **MS:** identified based on computer matching of the mass spectra with those of the Wiley and MassFinder libraries.

The Venn analysis revealed 99 distinct volatile constituents across the three oils (Fig 1). Seventeen compounds were common to all species, indicating the presence of a shared chemical core within the investigated taxa. However, substantial species-specific variation was also observed: 29 constituents were exclusive to *H. argaeum*, 17 to *H. platytaenium*, and 12 to *H. sphondylium* subsp. *ternatum*. Regarding pairwise overlap, ten constituents were shared exclusively between *H. platytaenium* and *H. sphondylium* subsp. *ternatum*, ten between *H. argaeum* and *H. platytaenium*, and only four between *H. argaeum* and *H. sphondylium* subsp. *ternatum*. The comparatively large number of compounds unique to *H. argaeum* is consistent with its monoterpene-rich composition and its clear chemical distinction from the two ester-dominated oils.

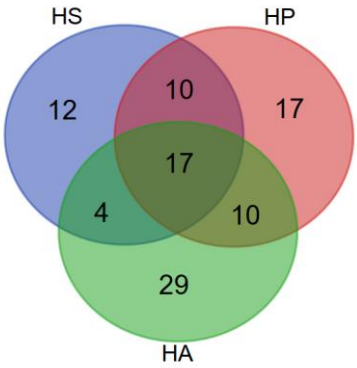


Fig 1. Venn diagram showing the distribution of volatile compounds identified in the essential oils

HA: *Heracleum argaeum*, **HP**: *H. platytaenium* **HS:** *H. sphondylium* subsp. *ternatum*

Previous studies have particularly emphasized the marked chemical variability among organs and populations of *Heracleum* taxa (Özek et al., 2005; Falahati-Anbaran et al., 2018; Ušjak et al., 2020). Fruit oils are frequently dominated by aliphatic esters, especially octyl acetate, octyl butyrate, and hexyl butyrate, whereas oils obtained from aerial parts, leaves, and flowers show broader variation involving monoterpenes, sesquiterpenes, phenylpropanoids, and aliphatic derivatives.

For *H. platytaenium*, the first two principal components explained 46.5% of the total variance, with PC1 and PC2 accounting for 24.0% and 22.5%, respectively. PCA differentiated the octyl acetate-rich oils, particularly the fruit oils of the EOs, from less common compositional profiles (Table 2, Fig 2, Fig 3). Most fruit oils from Tokat, Bursa, Kütahya, Isparta, and Manisa contained octyl acetate as the main compound, generally at concentrations above 70%. In contrast, the octyl butyrate-rich fruit oil (sample 7), the limonene/β-pinene-rich aerial oil (sample 14), the apiole- and elemicin-containing oil (sample 15), and the myristicin/octanol-containing oil (sample 18) showed distinct chemical patterns. The present aerial parts oil (sample 1) was also differentiated from the predominant fruit-oil group because of its high hexyl butyrate content. HCA supported this separation by grouping the octyl acetate-dominated oils and distinguishing the chemically atypical samples at lower similarity levels. The final amalgamation occurred at a similarity level of 30.2%, demonstrating considerable overall heterogeneity among the investigated *H. platytaenium* oils.

Table 2. The studies of EOs of *Heracleum platytaenium*

Part	Fig 2's PCA No	Location	Main compounds	Yield (%)	Ref.
Aerial parts	1	Kayseri-Türkiye	Hexyl butyrate (40.8%), octyl acetate (13.7%), methyl butanoate (10.6%)	0.1	Our study
Fruits	2	Tokat-Türkiye	Octyl acetate (87.6%)	5.3	Özek et al., 2005
Fruits	3	Tokat-Türkiye	Octyl acetate (87.8%)	-	Özek et al., 2005
Fruits	4	Tokat-Türkiye	Octyl acetate (84.8%)	-	Özek et al., 2005
Fruits	5	Tokat-Türkiye	Octyl acetate (85.6%)	4.9	Özek et al., 2005
Fruit	6	Tokat-Türkiye	Octyl acetate (87.6%)	5.33	İşcan et al., 2004

Fruits	7	Türkiye	Octyl butyrate (83.5%)	-	Özdemir et al., 2022
Fruits	8	Bolu-Türkiye	Octyl hexanoate (8.8%)	-	Yılmaz et al., 2021
Fruit	9	Bursa-Türkiye	Octyl acetate (72.3%), octyl butyrate (16.7%)	5.2	Kürkçüoğlu et al., 1995
Fruit	10	Kütahya-Türkiye	Octyl acetate (76.7%), octyl butyrate (11.3%)	6.8	Kürkçüoğlu et al., 1995
Fruit	11	Isparta-Türkiye	Octyl acetate (84.5%)	9.4	Tosun et al., 2026
Fruit	12	Isparta-Türkiye	Octyl acetate (90.1%)	8.7	Tosun et al., 2026
Fruit	13	Manisa, Türkiye	Octyl acetate (87.9%)	2.6	Özkırım et al., 2012
Aerial parts	14	Sinop-Türkiye	Limonene (30.8%), *β*-pinene (16.3%)	0.5	Elkıran et al., 2018
Aerial parts	15	Artvin-Türkiye	Octyl acetate (36.5%), apiole (24.9%), elemicin (20.8%)	-	Karan and Genç., 2018
Aerial parts	16	Samsun-Türkiye	Octyl acetate (85.5%)	-	Akçın et al., 2013
Roots	17	Trabzon-Türkiye	*p*-Cymene (33.9%), terpinolene (14.3%), *γ*-terpinene (7.1%)	4.0	Kılıç et al., 2016
-	18	Gümüşhane-Türkiye	Myristicin (27.5%), octyl acetate (25.1%), octanol (16.9%)	-	Bayan et al, 2016

-: not reported

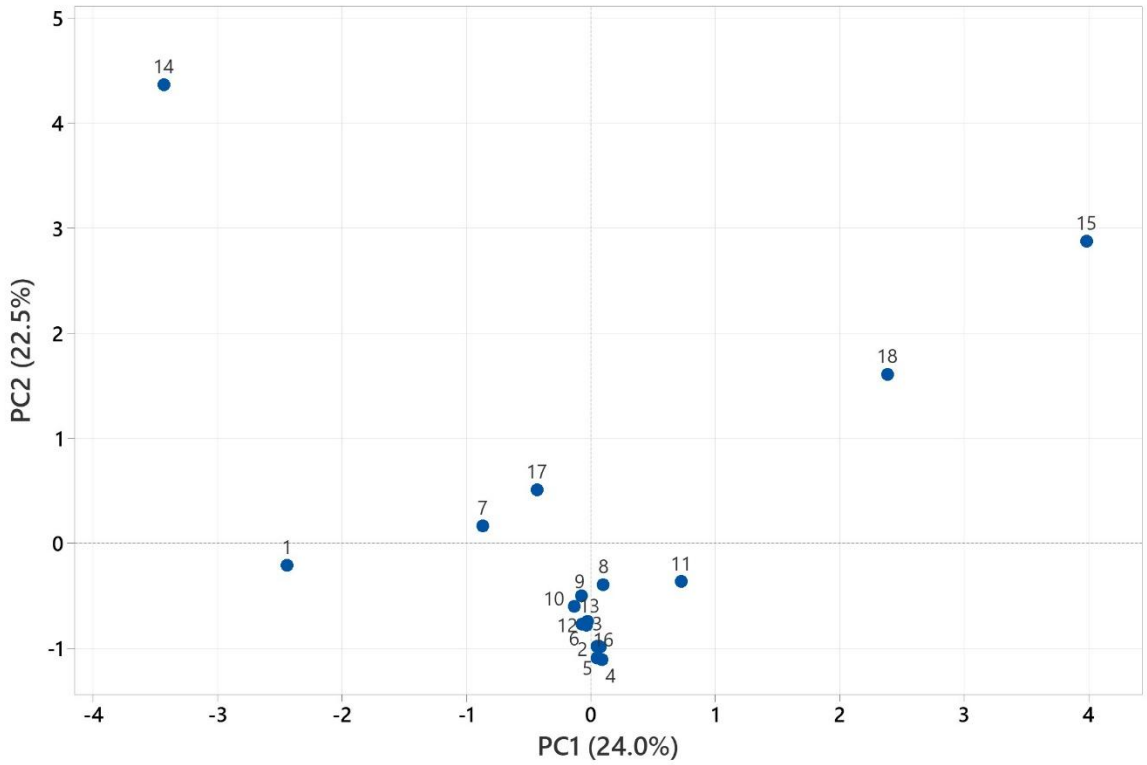


Fig 2. Principal component analysis of the essential oil compositions reported for *Heracleum platytaenium*

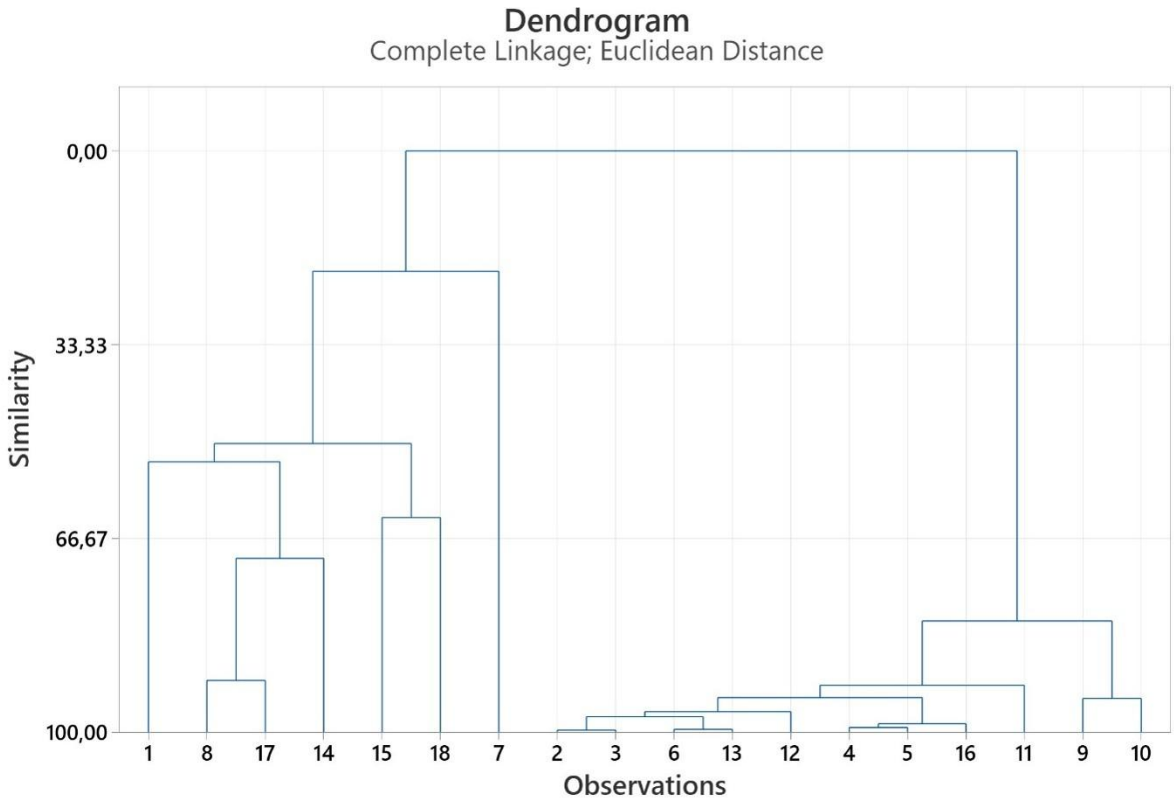


Fig 3. Hierarchical cluster analysis of the essential oil compositions reported for *Heracleum platytaenium*

For the oils included in **Table 3**, PC1 and PC2 explained 59.2% and 25.6% of the total variance, respectively, giving a cumulative contribution of 84.8% (Fig 4). The relatively moderate proportion represented by the first two components

indicates a multidimensional chemical structure rather than separation along a single dominant compositional gradient. The main group comprised samples characterised by octyl acetate and octyl butyrate, particularly the fruit oils of *H. sphondylium* subsp. *ternatum*. Octanol-rich samples 2 and 12 differed from this central ester-dominated pattern, while the myristicin-containing samples 13-15 formed another group of EOs. More pronounced differentiation was associated with bicyclogermacrene in sample 16, hexyl butyrate in sample 18, *(Z)-β*-ocimene and octanol in sample 20, sesquiterpene hydrocarbons and oxygenated sesquiterpenes in samples 21 and 22, and apiole in sample 23. HCA was consistent with the PCA pattern and separated the recurrent ester-related variables from the less frequent terpenoid and phenylpropanoid markers (Fig 5). The final similarity level was 25.1%, which was lower than that obtained for *H. platytaenium* and therefore indicated greater chemical heterogeneity within the oils evaluated in **Table 3**. This variation was associated particularly with differences among fruits, aerial parts, leaves, flowers, and roots, as well as among samples collected from Türkiye and different European regions.

Table 3. The studies of EOs of *Heracleum sphondylium*

Plant	Fig 4's PCA No	Part	Location	Main compound	Yield (%)	Ref.
H. sphondylium ssp. *ternatum*	1	Aerial parts	Konya-Türkiye	Octyl acetate (53.6%), octyl butyrate (18.5%)	0.18	our study
	2	Fruit	Denizli-Türkiye	Octanol (39.2%), octyl butyrate (27.4%), octyl acetate (10.6%)	3.7	Özek et al., 2002
	3	Fruit	Denizli-Türkiye	Octyl butyrate (42.9%), octyl acetate (30.9%)	-	Özek et al., 2002
	4	Fruit	Italy	Octyl acetate (61.0%), octyl butyrate (9.4%)	0.4	Pavela et al., 2018
	5	Fruit	Apennines-Italy	Octyl acetate (60.2%), octyl butyrate (10.1%)	0.4	Maggi et al., 2014
	6	Fruit	Montelago-Italy	Octyl acetate (54.9%), octyl butyrate (13.4%)	0.4	Maggi et al., 2014
	7	Fruit	Ankara-Türkiye	Octyl butyrate (37.7%), octyl acetate (31.6%), apiole (9.3%)	2.0	İşcan et al., 2004
	8	Fruits	Ankara-Türkiye	Octyl butyrate (37.7%), octyl acetate (31.6%), apiole (9.3%)	2.0	Özek et al., 2005
	9	Fruits	Ankara-Türkiye	Octyl acetate (38.5%), octyl butyrate (34.6%)	-	Özek et al., 2005
	10	Fruits	Ankara-Türkiye	Octyl butyrate (40.0%), apiole (20.4%), octyl acetate (19.2%)	-	Özek et al., 2005
	11	Fruits	Ankara-Türkiye	Octyl butyrate (41.1%), octyl acetate (25.4%), apiole (14.7%)	1.3	Özek et al., 2005
	12	Fruits	Denizli-Türkiye	Octanol (50.3%), octyl butyrate (24.6%)	3.7	İşcan et al., 2003
	13	Fruits	Ankara-Türkiye	Octyl acetate (73.7%), myristicin (8.9%)	4.4	Köse et al., 2025
H. sphondylium subsp. *montanum*	14	Aerial parts	Ankara-Türkiye	Octyl acetate (56.1%), myristicin (24.2%)	0.2	Köse et al., 2025

	15	Root	Ankara-Türkiye	Octyl acetate (57.1%), myristicin (13.8%)	0.2	Köse et al., 2025
	16	Aerial parts	Scotland	Octyl acetate (29.5%), bicyclogermacrene (31.6%)	0.15	Porrello et al., 2024
H. sphondylium subsp. *sphondylium*	17	Fruit	Brittany-France	Octyl acetate (66.6%)	0.7	Pavela et al., 2018
	18	Fruit	Norway	Hexyl butyrate (31.8%), octyl acetate (24.1%)	-	Falahati-Anbaran et al., 2018
H. sphondylium	19	Fruit	Slovenia	Octyl acetate (67.1%)	1.0	Ušjak et al., 2018
	20	Aerial parts	Slovenia	*(Z)*-*β*-Ocimene (28.9%), octanol (16.6%)	0.1	Ušjak et al., 2018
	21	Aerial parts	Serbia	*ar*-Curcumene (13.4%), *β*-sesquiphellandrene (11.9%), *β*-bisabolene (10.1%), caryophyllene oxide (9.2%)	0.02	Matejić et al., 2016
	22	Leaves	Slovenia	Germacrene D (11.0%), *β*-bisabolene (10.6%)	0.14	Ušjak et al., 2020
	23	Flowers	Slovenia	Apiole (16.8%)	0.12	Ušjak et al., 2020

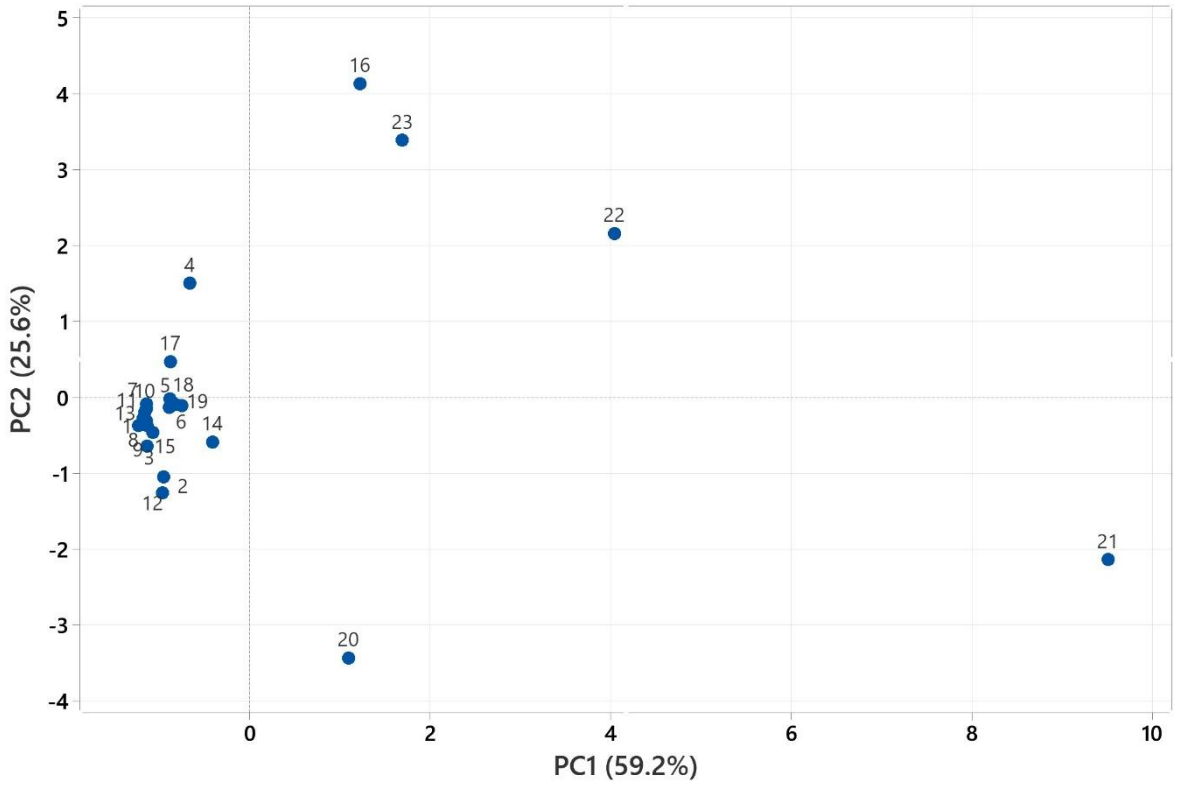


Fig 4. Principal component analysis of the essential oil compositions reported for *Heracleum sphondylium* and its subspecies

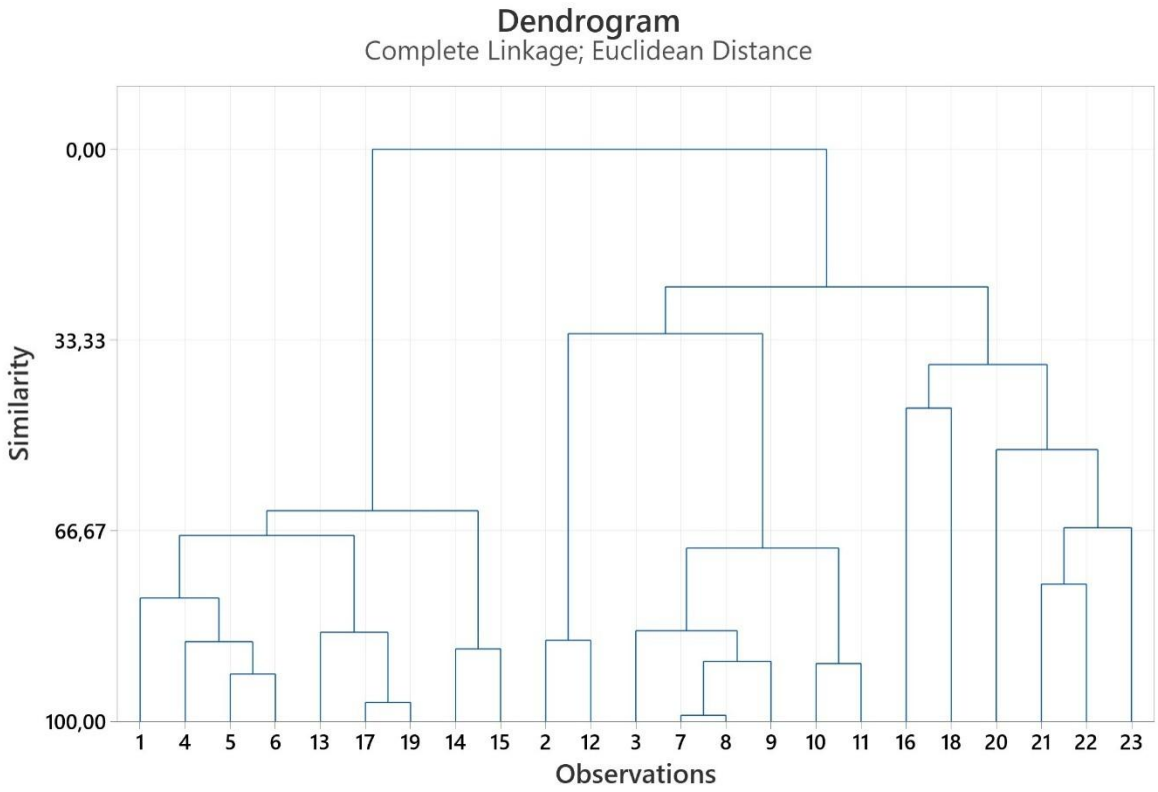


Fig 5. Hierarchical cluster analysis of the essential oil compositions reported for *Heracleum sphondylium* and its subspecies

The present *H. argaeum* aerial parts oil was characterised by a mixed monoterpene-ester profile in which *α*-pinene, *β*-pinene, limonene, hexyl butyrate, bornyl acetate, and *(E)*-*β*-ocimene were the principal constituents. This profile differed markedly from the previously investigated fruit oil, in which 69 constituents represented 96.4% of the total composition and hexyl butyrate was dominant at 39.1% (Başer et al., 1998). Albayrak et al. subsequently reported the detection of several volatile constituents in an essential oil obtained from the aerial parts of *H. argaeum*; however, only compound identities and retention times were presented, without their relative percentages (Albayrak et al., 2014). Consequently, a quantitative comparison with that study cannot be made. To the best of our knowledge, the present study provides the first detailed quantitative characterization of the essential oil from the aerial parts of *H. argaeum,* with 60 constituents identified and 95.1% of the total oil composition elucidated. The pronounced difference between the quantitatively characterized aerial parts oil and the previously reported fruit oil further demonstrates the importance of organ-associated variation in determining the essential-oil profile of *H. argaeum.*

Overall, the investigated oils exhibited low yields but high levels of chemical characterisation, with identified constituents accounting for 95.1-98.8% of their compositions. The results distinguished a monoterpene-rich *H. argaeum* oil from the aliphatic ester-rich oils of *H. platytaenium* and *H. sphondylium* subsp. *ternatum*. The Venn analysis demonstrated the coexistence of a shared volatile core and substantial species-specific diversity, while PCA and HCA showed that the literature samples were structured primarily by dominant chemical classes and sampled plant organs. These findings expand the available chemotaxonomic data for Turkish *Heracleum* taxa and demonstrate that species identity, organ selection, and geographical origin must all be considered when interpreting their essential-oil composition and potential biological properties.

Antimicrobial Activity

The antimicrobial activity of the essential oils of *Heracleum* species aerial parts was tested against reference Gram-positive bacteria, Gram-negative bacteria, and yeast strains. The results of the antimicrobial activity of the EOs are given in Table 4. From the results obtained, it is observed on a more pronounced activity against yeast than against Gram-negative bacteria and Gram-positive bacteria. Among the tested microorganisms, *C. krusei* was found to be more sensitive to the EOs of *Heracleum* species aerial parts.

Table 4. MIC Values (mg/mL) of Essential Oils of Heracleum Species

	Escherichia coli	***Staphylococcus aureus***	***Salmonella Tymphirium***	***Staphylococcus aureus***	***Candida albicans***	***Candida krusei***
H. sphondylium ssp. *ternatum*	>10	>10	10±0.00	>10	>5	2.5±0.72
H. argaeum	10	>10	>10	>10	>5	1.25±0.00
H. platytaenium	>10	2.5	>10	10±0.00	5±0.72	2.5±0.01
Ampicilin	0.01±0.01	0.63±0.38	0.013±0.01	0.02±0.01		
Clarithromycin	0.02±0.01	0.63±0.38	0.04±0.72	0.16±0.38		
Ketoconazole					0.01±0.01	0.04±0.01
Itraconazole					0.05±0.02	0.01±0.00
Fluconazole					0.07±0.03	0.03±0.01

Previous studies have examined the antimicrobial activity of essential oils obtained from the fruits, flowering aerial parts, and leaves of several *Heracleum* taxa using broth microdilution, agar disc or well diffusion, bioautography, and vapour-phase assays (İşcan et al., 2003; sçan et al., 2004; Hacıoğlu et al., 2006; Özkırım et al., 2012; Akçın et al., 2013; Albayrak et al., 2014; Maggi et al., 2014; Bayan et al., 2016; Matejić et al., 2016).

İşcan et al. 2003, reported that the fruit essential oil of *H. sphondylium* subsp. *ternatum* inhibited the tested human pathogenic bacteria at MIC values of 0.125-1.0 mg/mL and showed its strongest activity against the plant pathogens *Pseudomonas syringae* pv. *syringae*, *Xanthomonas campestris* pv. *phaseoli*, and *X. campestris* (MIC, 31.25 µg/mL) (İşcan et al., 2003). The same oil inhibited *C. albicans* at 0.5 mg/mL, and 1-octanol was identified as its principal bioactive constituent. In a subsequent study, the fruit oils of *H. crenatifolium*, *H. platytaenium*, and *H. sphondylium* subsp. *ternatum* exhibited their greatest anticandidal activity against *C. glabrata*, with an MIC of 0.25 mg/mL for all three oils, whereas MIC values against the other tested *Candida* strains generally ranged from 0.5 to 2.0 mg/mL (İşcan et al., 2003). Similarly, the aerial parts oil of *H. platytaenium* produced inhibition zones of 12-32 mm against *C. glabrata* but did not inhibit the tested bacterial strains(Akçın et al., 2013). In contrast, the aerial parts oil of *H. argaeum* showed only weak activity against *Bacillus brevis*, *B. cereus*, *C. albicans*, and *Saccharomyces cerevisiae* in an agar-well diffusion assay (Albayrak et al., 2014). Matejić et al. identified *B. cereus* as the most susceptible microorganism to the aerial parts oil of *H. sphondylium*, whereas *E. coli* and *Salmonella enteritidis* were not inhibited within the tested concentration range (Matejić et al., 2016). The fruit oil of *H. sphondylium* subsp. *ternatum* and its major esters were also examined by microdilution, although their antibacterial effects were not considered noteworthy (Maggi et al., 2014). In other biological models, *H. platytaenium* essential oil inhibited *Paenibacillus larvae*, the causative agent of American foulbrood disease, and its vapour phase

inhibited the mycelial growth of *Alternaria solani* and *Monilia laxa* by 77.63% and 59.63%, respectively, at 10 µL/Petri dish (Özkırım et al., 2012; Bayan et al., 2016). Collectively, these findings demonstrate that the antimicrobial effects of *Heracleum* essential oils vary markedly according to the plant organ, oil composition, test microorganism, and assay method. In the present study, *C. krusei* was the most susceptible microorganism to all three aerial parts oils, with the highest activity observed for *H. argaeum* oil (MIC, 1.25 mg/mL).

Molecular Docking Simulation

The reliability of the docking protocol was evaluated by redocking the co-crystallized ligand posaconazole (POSA) into the active-site cavity of *Candida albicans* lanosterol 14α-demethylase (CYP51; PDB ID: 5FSA). Among the 20 generated conformations, the second-ranked pose reproduced the crystallographic orientation with a heavy-atom root-mean-square deviation (RMSD) of 0.996 Å and a predicted binding affinity of -12.85 kcal/mol. The highest-scoring pose exhibited a slightly more favorable docking score of -12.97 kcal/mol but a higher RMSD of 2.651 Å. Thus, the docking procedure successfully retrieved a near-native POSA conformation among the two highest-ranked poses, although the native-like pose was not ranked first by the Vina scoring function.

Molecular docking analysis against Candida krusei CYP51

Nine volatile constituents representing the major components of the investigated *Heracleum* essential oils were docked into the binding cavity of the *C. krusei* CYP51 model. Their predicted binding affinities ranged from -5.349 to -6.733 kcal/mol (Table 5). Among the investigated compounds, *(-)*-limonene exhibited the most favorable docking score (-6.733 kcal/mol), followed by *(+)*-limonene (-6.713 kcal/mol), *(-)*-*α*-pinene (-6.577 kcal/mol), and *(-)*-*β*-pinene (-6.536 kcal/mol). The ester-type constituents displayed comparatively less favorable binding scores, with values of -5.774, -5.356, and -5.349 kcal/mol for octyl butyrate, octyl acetate, and hexyl butyrate, respectively.

The docking results revealed only minor stereoselective differences between the investigated enantiomeric pairs. The negative enantiomers produced slightly more favorable binding scores than their corresponding positive enantiomers. The differences were 0.058 kcal/mol for *α*-pinene, 0.081 kcal/mol for *β*-pinene, and 0.020 kcal/mol for limonene. These differences were too small to support a pronounced stereoselective preference based solely on the Vina scores. Nevertheless, the distinct interaction profiles observed for some enantiomeric pairs suggest that ligand stereochemistry influenced their predicted positioning within the CYP51 binding cavity.

Table 5. AutoDock Vina docking scores and principal PLIP-identified interactions of the investigated volatile constituents with the Candida krusei CYP51 model.

Ligand	Binding affinity (kcal/mol)	PLIP-identified interacting residues
(-)-Limonene	-6.733	Tyr72, Leu95, Leu96, Lys98, Pro233, Phe236, Val237, Phe380
(+)-Limonene	-6.713	Tyr72, Leu95, Lys98, Pro233, Phe236, Phe380
(-)-*α*-Pinene	-6.577	Tyr126, Leu129, Thr130, Tyr140, Phe231, Leu376
(-)-*β*-Pinene	-6.536	Tyr126, Leu129, Thr130, Tyr140, Phe231, Leu376

(+)-α-Pinene	-6.519	Phe134, Ile139
(+)-β-Pinene	-6.455	Phe134, Ile139
Octyl butyrate	-5.774	Tyr126, Thr130, Phe231, Leu376
Octyl acetate	-5.356	Tyr126, Thr130, Phe134, Phe231, Leu376
Hexyl butyrate	-5.349	Tyr126, Leu129, Thr130, Tyr140, Phe231, Leu376

Protein-ligand interaction profiling demonstrated that the binding of all nine volatile constituents was characterized exclusively by hydrophobic contacts, consistent with their predominantly nonpolar chemical structures (**Fig 6**). The number of hydrophobic contacts ranged from two to ten, with contact distances ranging from 3.41 to 3.98 Å. *(-)*-Limonene and *(+)*-limonene formed the highest numbers of hydrophobic contacts, with ten and nine contacts, respectively. Tyr126, Thr130, Phe231, and Leu376 were frequently involved in the binding of the pinene and ester-type constituents, whereas the limonene enantiomers predominantly interacted with a distinct group of residues, including Tyr72, Leu95, Lys98, Pro233, Phe236, and Phe380.

No hydrogen bonds, π-interactions, salt bridges, or direct metal coordination were identified by PLIP for any of the investigated constituents. None of the volatile compounds directly coordinated with the heme iron. Their predicted binding modes therefore appear to depend primarily on hydrophobic occupation of the *C. krusei* CYP51 binding cavity rather than the classical heme-coordination mechanism characteristic of azole antifungal agents.

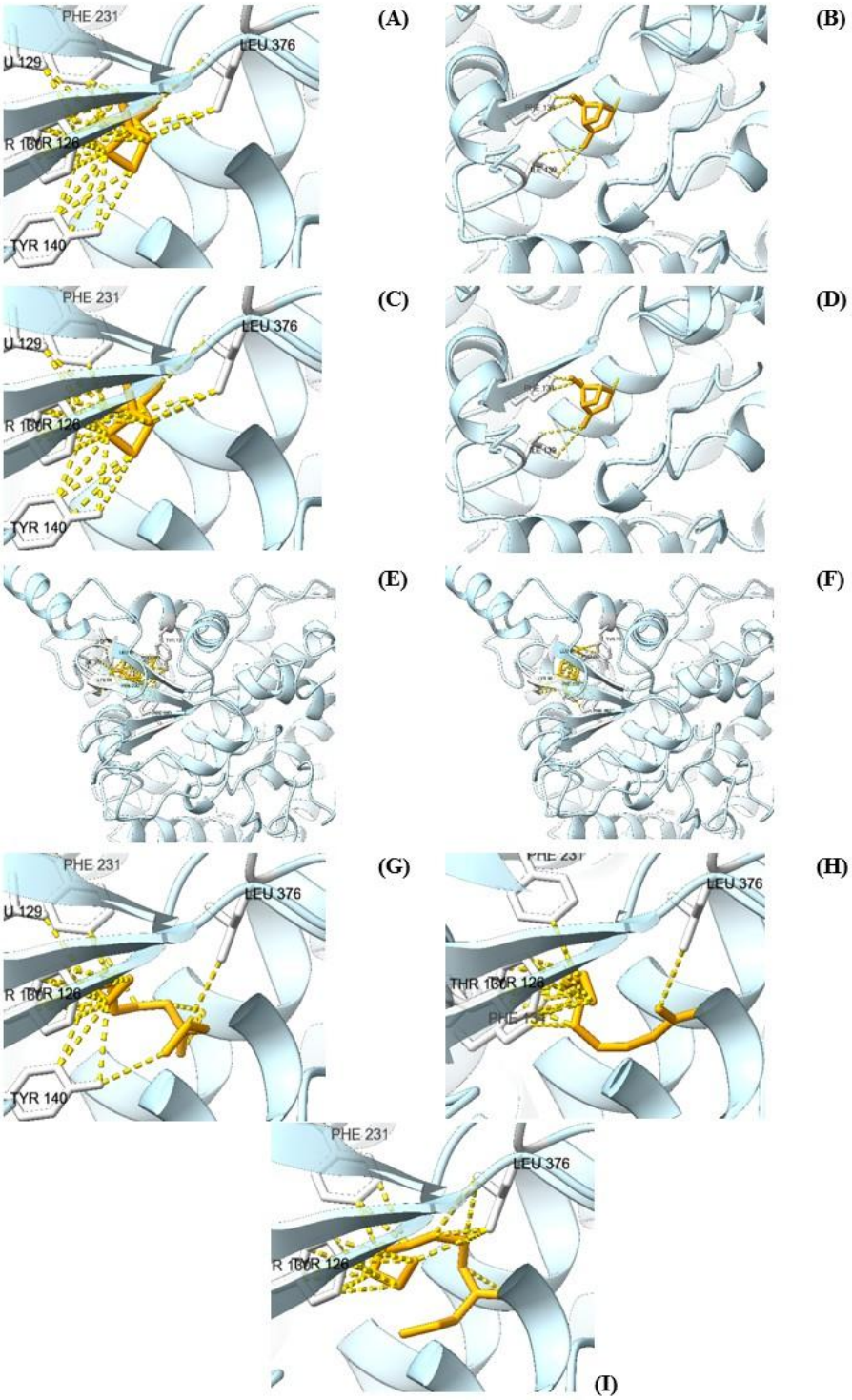


Fig 6. Predicted binding modes and PLIP-identified interactions of the investigated volatile constituents within the *Candida krusei* CYP51 model: **(A)** *(-)-α*-pinene, **(B)** *(+)-α*-pinene, **(C)** *(-)-β*-pinene, **(D)** *(+)-β*-pinene, **(E)** *(-)*-limonene, **(F)** *(+)*-limonene, **(G)** hexyl butyrate, **(H)** octyl acetate, and **(I)** octyl butyrate. Yellow dashed lines indicate hydrophobic contacts.

Molecular docking analysis against Candida albicans CYP51

The same nine volatile constituents were subsequently docked into the POSA-binding cavity of *C. albicans* CYP51. Their predicted binding affinities ranged from -5.148 to -6.821 kcal/mol (Table 6). Among the investigated compounds, (-)-limonene exhibited the most favorable docking score (-6.821 kcal/mol), followed by *(-)-β*-pinene (-6.735 kcal/mol), *(+)*-limonene (-6.696 kcal/mol), and *(-)-α*-pinene (-6.666 kcal/mol). The ester-type constituents showed comparatively less favorable binding scores, with values of -5.718, -5.331, and -5.148 kcal/mol for octyl butyrate, hexyl butyrate, and octyl acetate, respectively.

Modest stereoselective differences were also observed between the enantiomeric pairs. The negative enantiomers produced more favorable binding scores than their corresponding positive enantiomers. The differences were 0.202 kcal/mol for α-pinene, 0.219 kcal/mol for *β*-pinene, and 0.125 kcal/mol for limonene. Although relatively small, these differences were more pronounced than those observed for *C. krusei* and indicate that ligand stereochemistry affected the predicted accommodation of the monoterpenes within the *C. albicans* CYP51 cavity.

Table 6. AutoDock Vina docking scores and principal PLIP-identified interactions of the investigated volatile constituents with Candida albicans CYP51 (PDB ID: 5FSA).

Ligand	Binding affinity (kcal/mol)	PLIP-identified interacting residues
(-)-Limonene	-6.821	Tyr118, Ile304, Leu376
(-)-β-Pinene	-6.735	Phe126, Ile131, Tyr132, Phe228, Ile304
(+)-Limonene	-6.696	Ile131, Ile304, Leu376
(-)-α-Pinene	-6.666	Thr122, Phe126, Ile131, Tyr132, Phe228
(+)-β-Pinene	-6.516	Phe126, Ile131, Tyr132, Phe228, Ile304
(+)-α-Pinene	-6.464	Phe126, Ile131, Tyr132, Phe228, Ile304
Octyl butyrate	-5.718	Tyr118, Leu121, Phe126, Ile131, Tyr132, Leu376
Hexyl butyrate	-5.331	Tyr118, Phe126, Tyr132, Phe228, Leu376; H-bond with Tyr132
Octyl acetate	-5.148	Tyr118, Leu121, Thr122, Tyr132, Phe228

Protein-ligand interaction profiling showed that binding was predominantly stabilized by hydrophobic contacts, consistent with the largely nonpolar structures of the investigated volatile compounds (**Fig 7**). Phe126, Ile131, Tyr132, Phe228, Ile304, and Leu376 were among the most frequently involved residues. Hexyl butyrate was the only constituent for which PLIP identified a hydrogen bond, formed between one of its oxygen atoms and Tyr132 at 3.01 Å.

No direct coordination between the investigated volatile constituents and the heme iron was detected. Therefore, as observed by the *C. krusei* model, their predicted binding modes appear to depend principally on hydrophobic occupation of the CYP51 active-site cavity rather than direct heme coordination.

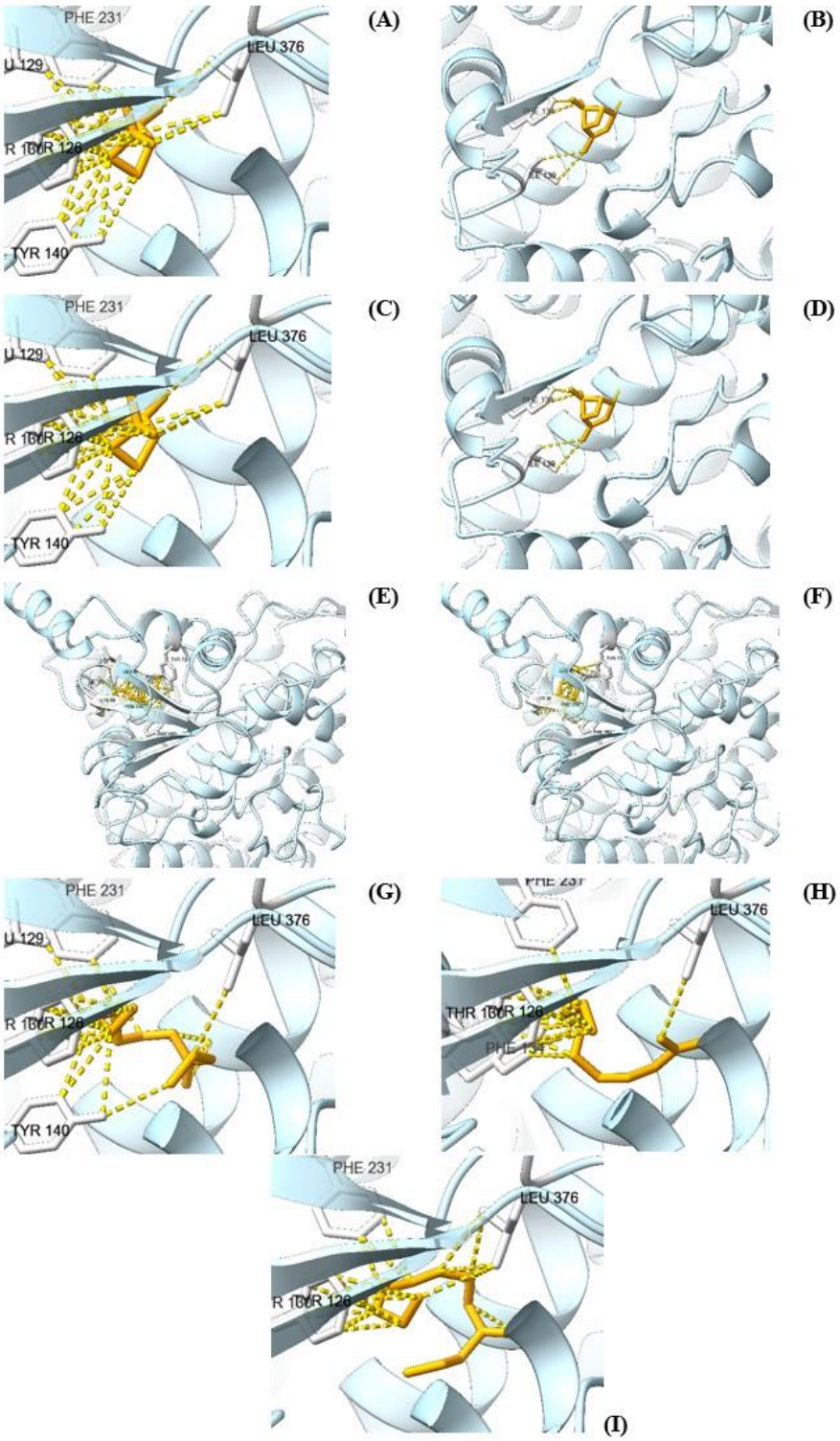


Fig 7. Predicted binding modes and PLIP-identified interactions of the investigated volatile constituents within *Candida albicans* CYP51 (PDB ID: 5FSA): **(A)** *(-)-α*-pinene, **(B)** *(+)-α*-pinene, **(C)** *(-)-β*-pinene, **(D)** *(+)-β*-pinene, **(E)** *(-)*-limonene, **(F)** *(+)*-limonene, **(G)** hexyl butyrate, **(H)** octyl acetate, and **(I)** octyl butyrate. Yellow dashed lines indicate hydrophobic contacts.

Comparative Evaluation of the Two Candida Strains

Overall, the investigated volatile compounds displayed comparable predicted affinities toward the CYP51 proteins of the two *Candida* species. The mean docking scores were -6.233 kcal/mol for *C. albicans* and -6.224 kcal/mol for *C. krusei*, indicating no meaningful overall difference in predicted binding strength. *(-)*-Limonene was the highest-scoring constituent against both targets, with values of -6.821 and -6.733 kcal/mol for *C. albicans* and *C. krusei*, respectively.

Despite the similarity in overall docking scores, species-dependent differences were observed in the predicted interaction patterns. The *C. albicans* complexes predominantly involved Phe126, Ile131, Tyr132, Phe228, Ile304, and Leu376. In the *C. krusei* model, the pinenes and ester-type constituents frequently interacted with Tyr126, Thr130, Phe231, and Leu376, whereas the limonene enantiomers occupied a region involving Tyr72, Leu95, Lys98, Pro233, Phe236, and Phe380. A hydrogen bond was detected only for the hexyl butyrate-*C. albicans* complex, while all interactions identified for *C. krusei* were hydrophobic.

The experimentally greater susceptibility of *C. krusei* was not reflected in the docking results. The mean Vina scores were similar for *C. krusei* and *C. albicans*, and no consistent relationship was observed between the experimental antifungal activity and the predicted docking scores. Therefore, the greater experimental susceptibility of *C. krusei* cannot be explained by the present CYP51 docking analysis. The docking results demonstrate only the predicted accommodation of the investigated volatile constituents within the CYP51 cavities and do not establish CYP51 inhibition as the mechanism underlying their antifungal activity. Experimental enzyme-inhibition or target-engagement studies would be required to confirm the involvement of CYP51.

ADMET Property Prediction

The physicochemical and pharmacokinetic profiles of the six major essential-oil constituents were evaluated using SwissADME and pkCSM (Table 7). Molecular weights ranged from 136.23 to 200.32 g/mol. All compounds lacked hydrogen-bond donors. The monoterpene hydrocarbons *α*-pinene, *β*-pinene, and limonene also lacked hydrogen-bond acceptors and had a topological polar surface area (TPSA) of 0.00 Å², whereas hexyl butyrate, octyl acetate, and octyl butyrate each contained two hydrogen-bond acceptors and had a TPSA of 26.30 Å². MLogP values ranged from 2.58 to 4.29, while ESOL logS values ranged from -3.50 to -2.43; all six compounds were classified as soluble by the ESOL model. α-Pinene and β-pinene each showed one Lipinski violation because MLogP exceeded 4.15, whereas limonene and the three ester constituents showed no Lipinski violations. The SwissADME bioavailability score was 0.55 for all compounds.

SwissADME classified *α*-pinene, *β*-pinene, and limonene as having low gastrointestinal absorption, whereas hexyl butyrate, octyl acetate, and octyl butyrate were classified as having high gastrointestinal absorption. Nevertheless, all six compounds were predicted to permeate the blood-brain barrier. The pkCSM predictions also supported substantial intestinal absorption, with human intestinal absorption values ranging from 93.748% to 98.770%, Caco-2 permeability values from 1.224 to 1.608 log Papp (10^{-6} cm/s), and BBB permeability values from 0.531 to 0.649 log BB. SwissADME classified all compounds as non-substrates of P-glycoprotein, while pkCSM classified the three monoterpene hydrocarbons as P-glycoprotein substrates and the ester constituents as non-substrates. These differences indicate model-dependent uncertainty in the predicted absorption and transporter profiles.

The pkCSM metabolism predictions identified *α*-pinene and *β*-pinene as potential CYP1A2 inhibitors. Limonene and the three ester constituents were not predicted to inhibit CYP1A2. None of the six compounds was predicted to be a CYP2D6 or CYP3A4 substrate, and no inhibition of CYP2C19, CYP2C9, CYP2D6, or CYP3A4 was predicted. Total-clearance

estimates were lower for the monoterpene hydrocarbons (0.041-0.224 log mL/min/kg) than for the ester constituents (1.597-1.687 log mL/min/kg), indicating compound-class differences in their predicted elimination profiles.

No compound was predicted to be AMES-positive, hepatotoxic, or an inhibitor of hERG I or hERG II. Skin-sensitisation alerts were obtained for limonene, hexyl butyrate, octyl acetate, and octyl butyrate, whereas α-pinene and *β*-pinene were predicted as non-sensitisers. The predicted maximum tolerated dose ranged from 0.558 to 1.259 log mg/kg/day. Oral rat acute-toxicity (LD_{50}) estimates ranged from 1.643 to 2.275 mol/kg, and chronic-toxicity (LOAEL) estimates ranged from 2.172 to 2.467 log mg/kg body weight/day. Overall, the *in silico* findings showed high intestinal-absorption estimates in pkCSM and consistent BBB-permeation predictions but also revealed compound- and model-dependent differences in transporter status, metabolism, clearance, and skin-sensitisation alerts. These results represent computational estimates and require experimental pharmacokinetic and toxicological confirmation.

Table 7. Physicochemical properties and ADME predictions of the main compounds in the essential oils based on SwissADME and pkCSM analysis.

	Compounds					
Predicted parameters	***α-Pinene***	***β-Pinene***	**Limonene**	**Hexyl butyrate**	**Octyl acetate**	**Octyl butyrate**
MW (g/mol)	136.23	136.23	136.23	172.26	172.26	200.32
NHD	0	0	0	0	0	0
NHA	0	0	0	2	2	2
NRB	0	0	1	8	8	10
TPSA (A^{o2})	0.00	0.00	0.00	26.30	26.30	26.30
MLogP lipophilicity	4.29	4.29	3.27	2.58	2.58	3.15
LogS (ESOL) water solubility	-2.48	-3.31	-3.50	-2.43	-2.53	-3.16
Lipinski's violation	1	1	0	0	0	0
ADME predictions						
GI absorption	Low	Low	Low	High	High	High
BBB permeability	Yes	Yes	Yes	Yes	Yes	Yes
Bioavailability score	0.55	0.55	0.55	0.55	0.55	0.55
Pharmacokinetic and toxicity predictions (pkCSM)						
Absorption						
Water solubility (log mol/L)	-3.665	-3.92	-3.608	-2.693	-3.136	-3.831
Caco-2 permeability (log Papp in 10^{-6} cm/s)	1.245	1.263	1.248	1.226	1.608	1.224
Intestinal absorption (human, %)	98.77	98.77	98.048	94.455	94.665	93.748

	Compounds					
Predicted parameters	***α-Pinene***	***β-Pinene***	**Limonene**	**Hexyl butyrate**	**Octyl acetate**	**Octyl butyrate**
Skin permeability (log Kp)	-1.791	-1.735	-1.5	-1.739	-1.694	-1.723
P-glycoprotein substrate	Yes	Yes	Yes	No	No	No
P-glycoprotein I inhibitor	No	No	No	No	No	No
P-glycoprotein II inhibitor	No	No	No	No	No	No
Distribution						
VDss (human, log L/kg)	0.775	0.748	0.503	0.052	0.115	0.149
Fraction unbound (human, Fu)	0.397	0.357	0.422	0.461	0.437	0.344
BBB permeability (log BB)	0.531	0.539	0.557	0.611	0.608	0.649
CNS permeability (log PS)	-1.84	-1.493	-2.006	-2.233	-2.214	-2.103
Metabolism						
CYP2D6 substrate	No	No	No	No	No	No
CYP3A4 substrate	No	No	No	No	No	No
CYP1A2 inhibitor	Yes	Yes	Yes	No	No	No
CYP2C19 inhibitor	No	No	No	No	No	No
CYP2C9 inhibitor	No	No	No	No	No	No
CYP2D6 inhibitor	No	No	No	No	No	No
CYP3A4 inhibitor	No	No	No	No	No	No
Excretion						
Total clearance (log mL/min/kg)	0.044	0.041	0.224	1.619	1.597	1.687
Renal OCT2 substrate	No	No	No	No	No	No
Toxicity						
AMES toxicity	No	No	No	No	No	No
Max. tolerated dose (human, log mg/kg/day)	1.035	1.143	1.259	0.761	0.558	0.612
hERG I inhibitor	No	No	No	No	No	No
hERG II inhibitor	No	No	No	No	No	No
Oral rat acute toxicity (LD50, mol/kg)	2.275	2.171	2.257	1.743	1.722	1.643

	Compounds					
Predicted parameters	***α-Pinene***	***β-Pinene***	**Limonene**	**Hexyl butyrate**	**Octyl acetate**	**Octyl butyrate**
Oral rat chronic toxicity (LOAEL, log mg/kg_bw/day)	2.172	2.246	2.204	2.338	2.431	2.467
Hepatotoxicity	No	No	No	No	No	No
Skin sensitisation	No	No	Yes	Yes	Yes	Yes
T. pyriformis toxicity (log ug/L)	0.525	0.66	0.213	0.825	0.848	1.594
Minnow toxicity (log mM)	0.94	0.612	1.132	0.727	0.584	0.192

NHD: Number of hydrogen donors; **NHA:** Number of hydrogen acceptors; **NRB:** Number of rotatable bonds; **TPSA:** Topological polar surface area; **GI:** Gastrointestinal, **BBB:** Blood brain barrier, **P-gp:** P-glycoprotein, **CYP:** Cytochrome; **HIA:** Human intestinal absorption.

MW, MLogP, LogS (ESOL), NHD, NRB, NHA, TPSA, Lipinski compliance, ESOL class, and bioavailability score were obtained from SwissADME. BBB log BB, CYP interaction, HIA, P-gp substrate and total clearance were obtained from pkCSM. All six compounds were classified as BBB-permeant by SwissADME.

Conclusions

In conclusion, this study integrated chemical profiling, antimicrobial evaluation, multivariate analyses, molecular docking, and ADMET prediction to characterise the essential oils of *H. argaeum*, *H. platytaenium*, and *H. sphondylium* subsp. *ternatum*. The results revealed species- and organ-dependent chemical differentiation and provided the first detailed quantitative characterisation of the aerial parts essential oil of *H. argaeum*. The observed antifungal activity, particularly against *C. krusei*, may partly reflect the individual or combined contributions of the major monoterpene hydrocarbons and aliphatic esters, including α-pinene, β-pinene, limonene, hexyl butyrate, octyl acetate, and octyl butyrate. However, the greater susceptibility of *C. krusei* was not directly correlated with stronger CYP51 binding, suggesting that these constituents may also act through membrane-related effects, additional cellular targets, or interactions within the complex oil matrix. Overall, these findings expand the chemotaxonomic and biological knowledge of Turkish *Heracleum* taxa.

Experimental Section

Plant Material and Isolation of the Essential Oil

The sources of *Heracleum* species are given in **Table 8**. The EOs were obtained by hydrodistillation using a Clevenger-type apparatus for 3 h. EOs of *Heracleum* species were stored at 4 °C in amber vials, and EOs were analyzed by GC-FID and GC-MS simultaneously. The yield of extraction was expressed as volume (ml) of EO per 100 g of plant dry matter (v/w). The yield of EOs is shown in **Table 1.**

Table 8. The Source of *Heracleum* Species

Plants	**Collection**	**Date**	**Coll. Number**

H. argaeum	KAYSERİ: Erciyes Dağı, Güney Yamaçlar, Kurumuş dere yatağı	24.07.2018	S. DOĞU 3037
H. platytaenium	KAYSERİ: Pınarbaşı, Yukarı Beyçayır Köyü civarı, Dere kenarı	24.07.2018	S. DOĞU 3038
H. sphondylium ssp. *ternatum*	KONYA: Selçuklu, Başarakavak Kasabası girişi, Dere kenarı, 1100m	22.07.2018	S. DOĞU 3036

Extraction

The essential oil was obtained by hydrodistillation using a Clevenger-type apparatus for 3 h. EOs of *Heracleum sphondylium* ssp. *ternatum H. argaeum, H. platytaenium* examined by GC-FID, and GC-MS, simultaneously.

Gas chromatography (GC) and Gas Chromatography-Mass Spectrometry (GC/MS)

Essential oils were analysed by GC using a Hewlett-Packard 6890 (Sem Ltd., Istanbul, Turkey) system, and an HP Innowax FSC column (60 m × 0.25 mm ∅, with 0.25 μm film thickness) was used with nitrogen at 1 ml/min. Initial oven temperature was 60 °C for 10 min, and increased at 4 °C/min to 220 °C, then remained constant at 220 °C for 10 min and increased at 1 °C/min to 240 °C. Injector temperature was set at 250 °C. Percentage composition of the individual components was obtained from electronic integration using flame ionization detection (FID) at 250 °C. *n*-Alkanes were used as reference points in the calculation of relative retention indices (RRI).

GC/MS analysis was performed with a Hewlett-Packard GCD (Sem Ltd., Istanbul, Turkey) system, and an Innowax FSC column (60 m × 0.25 mm, 0.25 μm film thickness) was used with helium. GC oven temperature conditions were as described above; split flow was adjusted at 50 ml/min, and the injector temperature was at 250 °C. Mass spectra were recorded at 70 eV. The mass range was from m/z 35 to 425 (Kırcı et al., 2025).

Components of Essential Oils Identification

The volatile components were identified by comparing their relative retention times (RRI) to those of authentic samples or by comparing their relative retention index to a series of *n*-alkanes. For identification, an in-house library (Library's Başer) and computer matching against commercial databases (Library's MassFinder software 4.0 and Wiley GC/MS Library (Wiley, NY, USA) were built up from actual components of known essential oil was employed (Köse et al., 2025).

Microbial Cultures

Essential oils of *Heracleum* species were tested using *Escherichia coli* NRRL B-3008 (Gr-), *Staphylococcus aureus* ATCC 6538 (Gr+), *Salmonella Typhimurium* ATCC 14028(Gr-), *Staphylococcus aureus* ATCC 700699(Gr+), *Candida albicans* ATCC 90028 and *C. krusei* ATCC 6258. Positive control agents were Ketoconazole (Fluka), itraconazole (FAGEM), Fluconazole (FAGEM) and Clarithromycin (Merck); ampicillin (Sigma) was used as standard antifungal and antibacterial agents, respectively.

Antimicrobial Activity

The microdilution broth susceptibility assay was used for the antibacterial and antifungal evaluation of the EOs. Stock solutions of the EO were prepared in dimethylsulfoxide (DMSO) and sterile distilled water. Overnight-grown microorganism suspensions in MHA (for bacteria) and *Candida* species yeast suspension in RPMI1640 (for fungus) were standardized to 108 CFU/mL. The wells were then filled with 100 µL of each culture suspension. The final row, which was devoid of microbes, served as sterility control. In another row, the microbe and MHA medium were used as growth control. The minimum inhibitory concentration (MIC, mg/mL) was obtained after a 24-hour incubation at 37°C. 20 µL of resazurin (Sigma) reagent was put on plates for visualization and incubated at 37°C for 3 hours (CLSI, 2006; Kırcı et al., 2023). All experiments were repeated three times, and average MICs were presented in Table 4.

Statistical analysis

GraphPad Prism Software Version 9.0 was used for data analysis to evaluate differences in results between the experimental and standard groups. The findings are displayed as the average ± standard deviation (S.D.). Original variables were defined as essential oil contents that exceeded 8.0% of the overall essential oils' compositions in at least one species. After normalization, the data were subjected to HCA and PCA. Minitab 19 was used to conduct statistical analysis (State College, PA, USA). Using the rescaled distances in the dendrogram and a cut-off point (Euclidean distance) that allows the attainment of consistent clusters, the number of clusters was computed. To determine the similarity among the essential oils regarding the contents of their chemical constituents, the PCA and the HCA were utilized. Additionally, to recognize volatile components of EOs, a Venn analysis was carried out (Kırcı et al., 2024; Köse et al., 2025).

In Silico ADMET Prediction of Main Compounds in Essential Oils

The *in silico* ADMET (Absorption, Distribution, Metabolism, Excretion, and Toxicity) analysis was performed to evaluate the pharmacokinetic profiles of the six main compounds (*α*-pinene, *β*-pinene, limonene, hexyl butyrate, octyl acetate, and octyl butyrate) identified in EOs. The canonical SMILES notations of all compounds were obtained from the PubChem database (https://pubchem.ncbi.nlm.nih.gov/). These SMILES strings were submitted to the SwissADME web tool (http://www.swissadme.ch/) to predict ADME-related molecular properties, drug-likeness, and medicinal chemistry parameters (Daina et al., 2017). Additionally, the absorption, distribution, metabolism, excretion, and toxicity (ADMET) profiles of the selected compounds were predicted using the pkCSM web server, which employs graph-based molecular signatures to estimate pharmacokinetic and toxicity properties (Pires et al., 2015).

Molecular Docking Analysis

The crystal structure of *Candida albicans* lanosterol 14α-demethylase (CYP51) complexed with posaconazole (POSA; PDB ID: 5FSA) was used as the experimental receptor (Hargrove et al., 2017). For *Pichia kudriavzevii* (syn. *Candida krusei*), the AlphaFold Protein Structure Database model AF-A0A142I6T1-F1, representing the full-length 528-residue ERG11/CYP51 protein, was used as the predicted receptor structure (Cock et al., 2009; Varadi et al., 2022). The model was structurally aligned with chain A of the experimentally determined *C. albicans* CYP51-POSA complex (PDB ID: 5FSA) using Biopython. Following structural alignment, the crystallographic heme coordinates of 5FSA were transferred to the corresponding CYP51 cavity of the *C. krusei* model and retained during rigid-receptor docking. The POSA-binding cavity of 5FSA was used as the structural reference for defining the docking region. Ligand three-dimensional structures were obtained from PubChem and converted to PDBQT format with Meeko 0.7.1; the receptors were prepared as rigid PDBQT files with the heme cofactor retained (Kim et al., 2016).

Docking was performed with AutoDock Vina 1.2.7 using the Vina scoring function, a grid centered at x = 191.504, y = 3.300, and z = 38.311 Å with dimensions of 27.402 × 33.865 × 23.010 Å, a grid spacing of 0.375 Å, exhaustiveness of 32, and 20 poses per ligand (Eberhardt et al., 2021). The protocol was validated by redocking POSA into 5FSA; the near-native pose showed a heavy-atom RMSD of 0.996 Å. The top-ranked pose of each volatile constituent was analyzed using the Protein-Ligand Interaction Profiler (PLIP), and the complexes were visualized in UCSF ChimeraX (Adasme et al., 2021; Pettersen et al., 2021).

Author Contribution Statement

D.K.: Conceptualization, investigation, formal analysis, data curation, writing the original draft; B.D., D.K.: formal analysis, data curation, writing-review & editing; B.D., D.K: formal analysis, writing the original draft; A.K., S.D.B.D., D.K.: supervision, writing- review & editing.

Funding Declaration

The authors declare that no financial support was received for the research, authorship, and/or publication of this manuscript.

References

Adasme M F, Linnemann K L, Bolz S N, Kaiser F, Salentin S, Haupt V J, Schroeder M (2021) PLIP 2021: Expanding the scope of the protein-ligand interaction profiler to DNA and RNA. Nucleic Acids Research 49:W530-W534. https://doi.org/10.1093/nar/gkab294

Akçın A, Seyis F, Akçın T A, Çaycı Y T, Çoban A Y (2013) Chemical composition and antimicrobial activity of the essential oil of endemic Heracleum platytaenium Boiss. from Turkey. Journal of Essential Oil Bearing Plants 16:166-171. https://doi.org/10.1080/0972060X.2013.793966

Albayrak S, Yurtseven L, Yaşar A, Aksoy A (2014) Chemical compositions of essential oil and in vitro biological activity of Heracleum argaeum Boiss. & Bal. Current Research in Biological and Pharmaceutical Sciences 3:1-6.

Bahadori M B, Dinparast L, Zengin G (2016) The genus Heracleum: A comprehensive review on its phytochemistry, pharmacology, and ethnobotanical values as a useful herb. Comprehensive Reviews in Food Science and Food Safety 15:1018-1039. https://doi.org/10.1111/1541-4337.12222

Başer K H C, Kürkçüoğlu M, Aytaç Z (1998) Composition of the essential oil of Heracleum argaeum Boiss. et Bal. Journal of Essential Oil Research 10:561-562. https://doi.org/10.1080/10412905.1998.9700971

Bayan Y, Yılar M, Onaran A (2016) Antifungal activity and chemical composition of the essential oil of Heracleum platytaenium Boiss. Egyptian Journal of Biological Pest Control 26:237-240.

Clinical and Laboratory Standards Institute. (2006) Methods for dilution antimicrobial susceptibility tests for bacteria that grow aerobically (7th ed.; CLSI document M7-A7). Wayne, PA.

Cock P J A, Antao T, Chang J T, Chapman B A, Cox C J, Dalke A, Friedberg I, Hamelryck T, Kauff F, Wilczynski B, de Hoon M J L (2009) Biopython: Freely available Python tools for computational molecular biology and bioinformatics. Bioinformatics 25:1422-1423. https://doi.org/10.1093/bioinformatics/btp163

Daina A, Michielin O, Zoete V (2017) SwissADME: A free web tool to evaluate pharmacokinetics, drug-likeness and medicinal chemistry friendliness of small molecules. Scientific Reports 7:42717. https://doi.org/10.1038/srep42717

Davis P H (1972) Flora of Turkey and the East Aegean Islands (Vol. 4, pp. 265-538). Edinburgh: Edinburgh University Press.

Dinçel D, Hatipoğlu S D, Gören A C, Topçu G (2013) Anticholinesterase furocoumarins from Heracleum platytaenium, a species endemic to the Ida Mountains. Turkish Journal of Chemistry 37:675-683. https://doi.org/10.3906/kim-1303-55

Eberhardt J, Santos-Martins D, Tillack A F, Forli S (2021) AutoDock Vina 1.2.0: New docking methods, expanded force field, and Python bindings. Journal of Chemical Information and Modeling 61:3891-3898. https://doi.org/10.1021/acs.jcim.1c00203

Elkıran Ö, Gül F (2018) Chemical composition of the essential oil of Heracleum platytaenium Boiss. (Apiaceae) growing wild in Turkey. Karaelmas Science and Engineering Journal 8:59-62. https://doi.org/10.7212%2Fzkufbd.v8i1.767

Falahati-Anbaran M, Mohammadi Bazargani M, Rohloff J (2018) Large-scale geographical mapping of essential oil volatiles in Heracleum (Apiaceae): Identification of novel compounds and unravelling cryptic variation. Chemistry & Biodiversity 15:e1800230. https://doi.org/10.1002/cbdv.201800230

Fırat M (2024) Heracleum kurdicum sp. nov. (Apiaceae), a new species from Hakkari (Turkey). Adansonia 46:223-237. https://doi.org/10.5252/adansonia2024v46a21

Hacıoğlu S (2006) Bazı Heracleum L. (Umbelliferae) taksonlarında uçucu yağların antimikrobiyal aktivitelerinin incelenmesi. Master's thesis, Kırıkkale University.

Hargrove T Y, Friggeri L, Wawrzak Z, Qi A, Hoekstra W J, Schotzinger R J, York J D, Guengerich F P, Lepesheva G I (2017) Structural analyses of Candida albicans sterol 14α-demethylase complexed with azole drugs address the molecular basis of azole-mediated inhibition of fungal sterol biosynthesis. Journal of Biological Chemistry 292:6728-6743. https://doi.org/10.1074/jbc.M117.778308

İşcan G, Demirci F, Kürkçüoğlu M, Kıvanç M, Başer K H C (2003) The bioactive essential oil of Heracleum sphondylium L. subsp. ternatum (Velen.) Brummitt. Zeitschrift für Naturforschung C 58:195-200. https://doi.org/10.1515/znc-2003-3-410

İşcan G, Özek T, Özek G, Duran A, Başer K H C (2004) Essential oils of three species of Heracleum: Anticandidal activity. Chemistry of Natural Compounds 40:544-547. https://doi.org/10.1007/s10600-005-0032-z

Karan T, Genç N (2018) Antioxidant activities of Heracleum platytaenium extracts and essential oil. Turkish Journal of Agriculture-Food Science and Technology 6:1274-1278. https://doi.org/10.24925/turjaf.v6i9.1274-1278.2040

Kılıç C S, Demirci B, Coşkun M, Başer K H C (2016) Chemical composition of Heracleum platytaenium Boiss. (Apiaceae) essential oil from Turkey. Natural Volatiles and Essential Oils 3:13-23.

Kim S, Thiessen P A, Bolton E E, Chen J, Fu G, Gindulyte A, Han L, He J, He S, Shoemaker B A, Wang J, Yu B, Zhang J, Bryant S H (2016) PubChem substance and compound databases. Nucleic Acids Research 44:D1202-D1213. https://doi.org/10.1093/nar/gkv951

Kırcı D, Demirci F, Demirci B (2023) Microbial transformation of hesperidin and biological evaluation. ACS Omega 8:42610-42621. https://doi.org/10.1021/acsomega.3c05334

Kırcı D, Kılıç C S, Duman H, Demirci B (2024) Biological activities and chemical compositions of Prangos platychlaena Boiss. essential oil and fractions: Multivariate statistical analyses. ACS Omega 9:11217-11222. https://doi.org/10.1021/acsomega.3c05700

Kırcı D, Özşen Batur Ö, Demirci B, Demirci F (2025) Synergistic antimicrobial effects of Melaleuca alternifolia essential oil and kojic acid combinations. Current Microbiology 82:192. https://doi.org/10.1007/s00284-025-04175-4

Köse T I, Yardımcı G B, Kırcı D, Polat D C, Demirci B, Eryılmaz M, Kılıç C S (2025) Bioactivities and chemotaxonomy of four Heracleum species: A comparative study across plant parts. Pharmaceuticals 18:576. https://doi.org/10.3390/ph18040576

Kürkçüoğlu M, Özek T, Başer K H C, Malyer H (1995) Composition of the essential oil of Heracleum platytaenium Boiss. from Turkey. Journal of Essential Oil Research 7:69-70. https://doi.org/10.1080/10412905.1995.9698465

Kurtul E, Küpeli Akkol E, Karpuz Ağören B, Yaylacı B, Bahadır Acıkara Ö, Sobarzo-Sánchez E (2025) Phytochemical investigation and assessment of the anti-inflammatory activity of four Heracleum taxa growing in Turkey. Frontiers in Pharmacology 15:1494786. https://doi.org/10.3389/fphar.2024.1494786

Maggi F, Quassinti L, Bramucci M, Lupidi G, Petrelli D, Vitali L A, Papa F, Vittori S (2014) Composition and biological activities of hogweed [Heracleum sphondylium L. subsp. ternatum (Velen.) Brummitt] essential oil and its main components octyl acetate and octyl butyrate. Natural Product Research 28:1354-1363. https://doi.org/10.1080/14786419.2014.904311

Matarrese E, Renna M (2023) Prospects of hogweed (Heracleum sphondylium L.) as a new horticultural crop for food and non-food uses: A review. Horticulturae 9:246. https://doi.org/10.3390/horticulturae9020246

Matejić J S, Džamić A M, Mihajilov-Krstev T, Ristić M S, Ranđelović V N, Krivošej, Z Đ., Marin P D (2016) Chemical composition, antioxidant and antimicrobial properties of essential oil and extracts from Heracleum sphondylium L. Journal of Essential Oil Bearing Plants 19:944-953. https://doi.org/10.1080/0972060X.2014.986538

Özdemir F G G, Tosun B, Şanlı A, Karadoğan T (2022) Bazı Apiaceae uçucu yağlarının Meloidogyne incognita (Kofoid & White, 1919) Chitwood, 1949 (Nematoda: Meloidogynidae)'ya karşı nematoksik etkisi. Ege Üniversitesi Ziraat Fakültesi Dergisi 59:529-539. https://doi.org/10.20289/zfdergi.1092623

Özek T, Demirci B, Başer K H C (2002) Comparative study of the essential oils of Heracleum sphondylium ssp. ternatum obtained by micro- and hydro-distillation methods. Chemistry of Natural Compounds 38:48-50. https://doi.org/10.1023/A:1015777614626

Özek T, Özek G, Başer K H C, Duran A (2004) Comparison of the essential oils of three endemic Turkish Heracleum species obtained by different isolation techniques. Journal of Essential Oil Research 17:605-610. https://doi.org/10.1080/10412905.2005.9699009

Özkırım A, Keskin N, Kürkçüoğlu M, Başer K H C (2012) Evaluation of some essential oils as alternative antibiotics against American foulbrood agent Paenibacillus larvae on honey bees Apis mellifera L. Journal of Essential Oil Research 24:465-470. https://doi.org/10.1080/10412905.2012.703504

Pavela R, Maggi F, Cianfaglione K, Bruno M, Benelli G (2018) Larvicidal activity of essential oils of five Apiaceae taxa and some of their main constituents against Culex quinquefasciatus. Chemistry & Biodiversity 15:e1700382. https://doi.org/10.1002/cbdv.201700382

Pettersen E F, Goddard T D, Huang C C, Meng E C, Couch G S, Croll T I, Morris J H, Ferrin T E (2021) UCSF ChimeraX: Structure visualization for researchers, educators, and developers. Protein Science 30:70-82. https://doi.org/10.1002/pro.3943

Pires D E V, Blundell T L, Ascher D B (2015) pkCSM: Predicting small-molecule pharmacokinetic and toxicity properties using graph-based signatures. Journal of Medicinal Chemistry 58:4066-4072. https://doi.org/10.1021/acs.jmedchem.5b00104

Porrello A, Merra R, Badalamenti N, Bruno M (2024) Heracleum sphondylium L. subsp. sphondylium (Apiaceae) of the Isle of Skye (Scotland): The chemical composition of essential oil from the flowering aerial parts. Natural Product Research 38:2920-2925. https://doi.org/10.1080/14786419.2023.2241147

Tosun B, Saraç Sivrikaya I, Güller A, Jabran K (2026) Essential oil composition and antifungal activity of Heracleum platytaenium Boiss. (endemic) fruits against soilborne pathogens. Journal of Essential Oil Bearing Plants, 1-8. https://doi.org/10.1080/0972060X.2026.2705487

Ušjak L J, Drobac M M, Niketić M S, Petrović S D (2018) Chemosystematic significance of essential oil constituents and furanocoumarins of underground parts and fruits of nine Heracleum L. taxa from Southeastern Europe. Chemistry & Biodiversity 15:e1800412. https://doi.org/10.1002/cbdv.201800412

Ušjak L, Niketić M, Drobac M, Petrović S (2020) Chemosystematic evaluation of leaf and flower essential oils of eight Heracleum taxa from Southeastern Europe. Plant Systematics and Evolution 306:4. https://doi.org/10.1007/s00606-020-01645-z

Uysal A, Özer O Y, Zengin G, Stefanucci A, Mollica A, Picot-Allain C M N, Mahomoodally M F (2019) Multifunctional approaches to provide potential pharmacophores for the pharmacy shelf: Heracleum sphondylium L. subsp. ternatum (Velen.) Brummitt. Computational Biology and Chemistry 78:64-73. https://doi.org/10.1016/j.compbiolchem.2018.11.018

Varadi M, Anyango S, Deshpande M, Nair S, Natassia C, Yordanova G, Yuan D, Stroe O, Wood G, Laydon A, Žídek A, Green T, Tunyasuvunakool S, Petersen S, Jumper J, Clancy E, Green R, Vora A, Lutfi M, Figurnov M, Cowie A, Hobbs N, Kohli H, Kleywegt G J, Birney E, Hassabis D (2022) AlphaFold Protein Structure Database: Massively expanding the structural coverage of protein-sequence space with high-accuracy models. Nucleic Acids Research 50:D439-D444. https://doi.org/10.1093/nar/gkab1061

Yılmaz A, Çiftçi V (2021) Determination of essential oil composition of naturally growing Heracleum platytaenium L. plant in Bolu ecological conditions. ISPEC Journal of Agricultural Sciences 5:344-349. https://doi.org/10.46291/ispecjasvol5iss2pp344-349

Supplementary Files

This is a list of supplementary files associated with this preprint. Click to download.

- Graphicalabstract.jpg